

Dust modeling using MODIS data and WRF-Chem and HYSPLIT models (Case study of dust storm from December 16 to 20, 2016)

Farshad Soleimani Sardo^{a*}, Nir Krakauer^b

^a Department of Ecological Engineering, Faculty of Natural Resources, University of Jiroft, Kerman, Iran

^b Department of Civil Engineering, The City College of New York, New York, United States of America (USA)

ABSTRACT

Dust storms cause major problems for human societies in arid and semi-arid regions. This phenomenon involves the transport of suspended particles in the atmosphere, often over long distances. In this study, MODIS data and WRF-Chem and HYSPLIT models were used to investigate aerosol optical depth (AOD) during a dust storm affecting Iran from December 16 to 20, 2016. The results showed that the output of the HYSPLIT model in the forward method for December 16, 2016, at 12 UTC, showed that the particles originating from this section, including the Jazmurian region, mainly moved south during this period. Also, the results showed that the AOD values in the south of Sistan and Baluchistan province and the border between Afghanistan and Pakistan, west of the Oman Sea, and east of the Persian Gulf show a significant increase compared to before. Also, the amount of this quantity has increased for the Jazmurian region and has reached 0.8 in some areas.

ARTICLE INFO

Keywords:

AOD index
Dust storm
Jazmurian basin
MODIS
WRF-Chem

Article history:

Received: 21 December 2024
Accepted: 29 January 2025

*Corresponding author

E-mail address:
f.soleimani@ujiroft.ac.ir
(F. Soleimani Sardo)

Citation:

Soleimani Sardo, F. & Krakauer, N., (2026). Evaluation of pollution indices in deposited dust (Case study; Qayen cement factory, Iran). *Sustainable Earth Trends*: 6(1), (55-65).

DOI: [10.48308/set.2025.238019.1098](https://doi.org/10.48308/set.2025.238019.1098)

1. Introduction

One of the most important sources of air pollution is dust storms. These storms carry a large amount of dust particles with them and affect human health and create problems for them (Dey et al., 2004; El-Askary et al., 2006). Dust storms can transport suspended particles in the atmosphere, sometimes thousands of kilometers, so the identification of collection sources is sometimes very far away, which can be a source of dust collection even in other continents (Tegen and Fung, 1994; Ginoux et al., 2001; Prospero et al., 2002; Prospero and Lamb, 2003; Mahowald et al., 2005; Uno et al., 2006; Li et al., 2008). These dust particles can change the optical properties of airborne particles as well as air quality. Its harmful effects

occur on a local to regional scale (e.g., Dey et al., 2004; Prasad et al., 2007; Zhao et al., 2010, 2011; Han et al., 2011; Kalenderski et al., 2013). Therefore, identifying and studying dust storms is of great importance. Wind is a fluid, so numerical models and satellite images should be used to study dust storms. Due to the nature of the atmosphere, and the impossibility of considering all real conditions in numerical models, the limitation of computing power, the existence of uncertainty in the simulation results of numerical models have always existed, and in recent years, efforts have been made to use the obtained advances to Different methods should be developed in different parts of numerical models to reduce uncertainty as much



as possible. In the current situation, the used numerical models often have scientifically acceptable errors and the accuracy of these models has reached such a level that their output is used for operational purposes. One of these models is WRF-Chem. The WRF-Chem model is used to simulate the concentration and transport of dust. This model can be used to simulate and predict the concentration of suspended particles in the atmosphere caused by natural mechanisms, human activities (pollutants) and dust in different sizes and how their publication and deposit should be used. In a study, [Hossein Hamzeh et al. \(2015\)](#) using synoptic station data as well as MODIS satellite images and the WRF-Chem numerical model investigated the synoptic and dynamic dust phenomenon and its simulation in the southwest of the country in the summer of 2014, the results showed that the areas The Syrian desert is the source of dust in the region. Also, [Kermani et al. \(2016\)](#) in a study, using MODIS satellite images, analyzed satellite images of fine dust and dust storms in Iran in order to investigate internal and external sources and their control methods. The results showed that the recent droughts, climate changes and global warming in the region are the most important natural causes of the dust phenomenon and some other factors such as the drying up of wetlands in the region and their destruction, the low percentage of vegetation in some areas prone to dust, the construction of large dams On the part of Turkey, the unstable development caused by the issue of war and the destruction of the Persian Gulf region has increased the intensity and scope of the dust phenomenon and caused it to spread to most of the regions of Iran. In this regard, [Kargar et al. \(2015\)](#) used the WRF-Chem model to simulate severe sand and dust storms in eastern Iran. MODIS satellite images and GOCART schematics were used in this study. [Nabavi et al., \(2016\)](#) investigated the climatology of dust distribution in West Asia using homogenized satellite and remote sensing data. Based on the results, the dust sources of areas on the border of Iraq and Saudi Arabia and recently in the northwest of Iraq were identified using MODIS images. [Rizza et al., \(2018\)](#) in order to evaluate the sensitivity of the WRF-Chem model to the earth surface models or models investigated several dust events in the Apulia region in the central Mediterranean. In this research, they

used three earth surface models named NOAH, RUC and NOAH They used Noa-MP. The results showed that the combination of WRF-Chem model with RUC land surface model is better in showing the amount of dust elements and minerals, on the other hand, the combination of this model with NOAH and Noah-MP is more suitable for showing PM₁₀. Also, [Kim et al., \(2017\)](#) developed a dust dynamic function model with high resolution in a study with dust storms in a regional model. They used the NU-WRF model and also used MODIS images and NDVI vegetation index. The results showed that the NU-WRF model can successfully investigate and track dust storms that could not be tracked by previous models. One of the most important indices for evaluating the intensity and concentration of dust is the AOD index, which can be estimated using MODIS satellite data. The AOD index has been studied in Jazmurian Basin. The Aerosol Optical Depth index is one of the most widely used indices to investigate the air pollution of different regions, especially dry and desert regions. Today, the use of satellite images and data has been expanded in order to investigate the condition of deserts and evaluate the places prone to the production of dust masses. MODIS sensor is one of the five sensors based on TERRA and AQUA satellites. MODIS sensor data can be used to obtain information such as temperature, atmospheric humidity, cloud cover and its properties, characteristics of aerosols, land and sea surface temperatures, natural and artificial fires, distribution and depth of ice and snow, ocean color, vegetation indices ([Gupta et al., 2008](#)). Optical depth (AOD) is a criterion that expresses the attenuation of the radiance entering the atmosphere due to absorption and interaction by suspended particles in a vertical column. Optical depth can be calculated using satellite data. This criterion can be used as an indirect estimate of the density of atmospheric particles. MODIS satellite data can be used for spatial and temporal analysis of optical depth ([Prasad et al., 2004](#)). In order to track and evaluate dust storms in the cities of Ahvaz and Kermanshah in the west of Iran, [Rajaei et al. \(2020\)](#) performed modeling in the HYSPLIT system by analyzing the return path at three levels of height to determine the direction of movement of suspended particles in the atmosphere and its origin at a distance of 48 the

hour before the occurrence of the dust storm should be determined. The comparison of the dust transmission routes produced by the HYSPLIT model for two destinations and the composition of dust false color identified in MODIS images showed similar sources for the dust phenomenon. Therefore, the primary sources of dust in the two cities of Ahvaz and Kermanshah, the desert parts of northern Iraq, an area between latitudes 33.80 to 35.35 degrees north and longitudes 42.00 to 46.44 degrees east were in the Tigris and Euphrates alluvial plains (Rajaei et al., 2020). Omidvar et al. (2022) in evaluating the relationship between aerosol optical depth (AOD) index, wind speed and visibility in dust storms using genetic algorithm in the central regions of Iran using evolutionary genetic algorithm (GA) mathematical relationship between the above parameters and wind speed (WS) were analyzed as a key index in the storm. In order to reach a mathematical equation, linear regression and several other famous functions were compared. Meanwhile, the binomial function was chosen as the best fitness function. The result of a mathematical equation between the parameters of AOD, visibility and wind speed during the occurrence of synoptic code 30-35 was based on a binomial function with a confidence level of 95% (Omidvar et al., 2022). In a research, the spatial and temporal variability of aerosol optical depth (AOD) at 550 nm was investigated over a period of 18 years (2000 to 2017) in the territory of China. The spatial distribution of AOD showed certain geographical differences with a gradual decrease from east to west of the country. Also, the seasonal variation of weather in most regions of China has maximum AOD in spring or summer and minimum in autumn or winter (Filonchik et al., 2019). Tavakoli Neko et al. (2024) identified and tracked dust and determined its origin in Qom province using MODIS satellite data and AOD index. The results showed that the maximum AOD index of about 2.3 and 2.24 was observed for the years 2018 and 2015, respectively. and it was concentrated mostly in the eastern and northern parts of the central part. The purpose of this study is the numerical analysis of the dust storm from December 16 to 21, 2016 in the Jazmurian region using MODIS satellite data and the WRF-Chem numerical model in order to prepare spatial maps of the AOD index.

2. Material and methods

2.1 Study area

The Jazmurian watershed with an area of 69,600 km² is considered a part of the middle-blocked basin of Iran in terms of division. The western half of this area with an area of 35,600 km² is located in Kerman province, and its eastern half with an area of 34,000 km² is located in Sistan and Baluchistan province. Due to the climate change phenomenon in recent years and the construction of numerous dams on its watershed, the Jazmurian wetland has suffered drought and has been identified as one of the centers of dust in the southeast of Iran. Due to the lack of suitable vegetation in the area, severe floods occur during the rains. Lack of vegetation causes the water from rains to penetrate less into the ground and promotes severe soil erosion. The amount of annual rainfall in the northern heights of the Jazmurian basin fluctuates between 500 and 600 mm, while in the broad and low southern part, the amount of rainfall does not exceed about 100 mm per year (Kardan et al., 2009). Although the Jazmurian watershed is a part of Iran's central watershed from a hydrological point of view, in terms of climatology it has exceptional and independent conditions from the central regions of Iran due to receiving abundant relative humidity from the Oman Sea; For this reason, despite the limitation of atmospheric precipitations, exhausting heat and very high annual potential evaporation, which is more than 4500 mm in some areas, in terms of the possibility of revitalization and reconstruction and exploitation of renewable natural resources, this area has good facilities compared with other central areas of Iran (Negaresh and Latifi, 2009). The location of the area is shown in Fig. 1.

2.2 Methods

In this research, Aqua Modis satellite images were used for December 19, 2016 to visualize the dust storm and HYSPLIT software was also used to understand the transport route of dust particles. These were also compared to the WRF-Chem simulation of the dust storm.

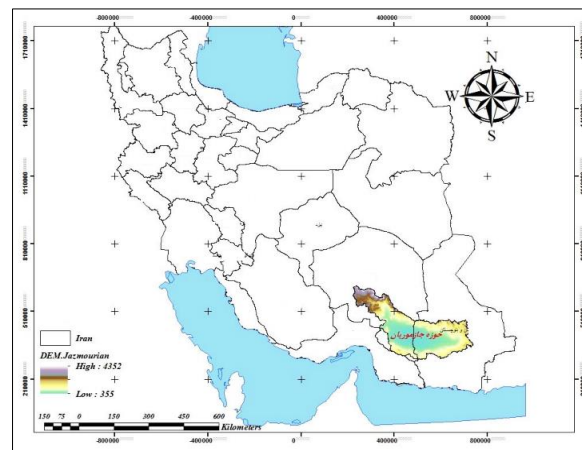


Fig. 1. Geographical location of the study area.

2.2.1 Dust storm routing using HYSPLIT model

The HYSPLIT model was designed by Draxler and Hess in 1997 and has been improved over the past few decades. This model is actually a dual model for dust movement calculations, dispersion and simulation of particle deposition using puff and particle approaches. This model is used to simulate the dust trajectory and identify the origin areas as well as the areas affected by the dust storm. The calculation method of the model is a combination of Eulerian and Lagrangian perspectives, and for this reason HYSPLIT is called a dual model. In order to determine the path of dust movement by this model, gridded meteorological data is needed. The minimum data required to analyze the movement path of dust is the orbital and meridional component of the wind, the vertical velocity (ω) and the geopotential height in a reference level. Several types of data are used for the input of the model, which in the study area is the only possibility to use GDAS data. GDAS is a global data set with two grids, one grid with a resolution of 1 degree and the other with a resolution of 0.5 degrees and are available for every three hours. GDAS data are available at 1° resolution since 2006 and 0.5° resolution since September 2007. Using data with a lower resolution will make the output of the model more accurate.

2.2.2 Characterization of dust storm using remote sensing

One of the ways to detect and identify the phenomenon of dust is remote sensing technology, and based on this technology, it is possible to help identify the sources of production and the path of fine dust, it was observed through previous studies that Modis

images have a high ability to detect It has dust, and in most cases, the index was used to detect fine dust, and the main reason is that the images related to the Madis sensor, in addition to highlighting the dust, have many spectral bands and have a suitable time step. Further, using MODIS satellite images and remote sensing methods, the dust in the studied area was revealed. MODIS data was downloaded from <https://search.earthdata.nasa.gov/search/granules>. MODIS sensor is installed on two satellites, Aqua and Terra, with 36 spectral bands in the wavelength range of 0.405 μm to 14.835 μm . Spatial resolution is 250 meters in bands 1 and 2, 500 meters in bands 3 to 7, and 1000 meters in bands 8 to 36. This scanner has almost universal coverage due to its large sampling width and 110 degree scanning angle. Madis images have a high capability for extracting ground surface temperature, vegetation cover and snow cover. 36 MODIS bands are designed for atmospheric-terrestrial and oceanographic studies, and 7 bands are intended for terrestrial applications. One of the characteristics of MODIS images is the high spectral resolution, which allows combining different bands and creating false color images to detect complications. Due to the high spectral and spatial resolution, the special calibration method and the narrowness of most of the spectral bands of this meter, which prevents the spectral absorption of water vapor in the infrared band and, as a result, the error caused by water vapor absorption is negligible; Therefore, the calculation accuracy in determining indicators such as vegetation cover (NDVI) increases. This sensor is superior to many sensors (Landsat and AVHRR). [Table 1](#) shows the bands that will be used in this study.

Table 1. Specifications of the spectral bands used to highlight dust on MADIS images.

Application	Band number	Wavelength (nm)	Bandwidth (nm)	Spatial resolution (m)
Boundaries/ aerosol/ cloud/ land	1	645	620-670	250
	2	858.5	841-876	
Characteristics of aerosols/clouds/land	3	469	459-479	300
	4	555	545-565	
Cloud/surface temperature	31	11030	10780-11280	
Cloud/surface temperature	32	12020	11770-12270	

2.2.3 Brightness temperature

Atmospheric temperature is the temperature recorded by the gauge, which is different from the surface temperature of the earth. The temperature of the earth's surface refers to the temperature of phenomena. But the brightness temperature is the temperature recorded by the meter and there is also the effect of the atmosphere. Luminosity temperature, which is the temperature corresponding to the radiant energy received from the surface by the sensor and calculated without considering the emissivity, is obtained from the inverse of Planck's equation (Eq. 1).

$$D = (BT_{31} - BT_{32}) \quad \text{Dust} < 0\mu\text{m} \quad (1)$$

The brightness temperature is different from the actual temperature. If the brightness temperature is considered as the surface temperature, it means that the atmospheric path has no effect on the amount of radiation and the surface is emitting radiation as a black body. In order to highlight the dust, the MODIS images downloaded on the mentioned dates in HDF format were entered into the ENVI5.1 software environment, and in the next step, to perform geometric corrections and calculate the brightness temperature of the desired bands from the MODIS Toolkit, which is installed on the ENVI5.1 software. After receiving the MODIS satellite data and performing the necessary pre-processing on them, Ackerman's BTM method was used to identify dust and applied to the image. For dust storms, Ackerman observed the difference in brightness temperature of band 31 (11 μm) and band 32 (12 μm) and proposed a threshold of zero ($\text{Dust} \leq 0$) as the global dust detection threshold values less than zero indicate dust.

In Ackerman's method, the difference in brightness temperature related to dust storms in bands 31 and 32 (wavelength 11 and 12 μm) of less than zero degrees Kelvin is chosen as the threshold for separating dust from other phenomena. The results of Ackerman's index

are shown in the figures, and the highlighted dust mass has been determined. Ackerman (1997) considered BTM (brightness temperature difference) values less than zero degrees Kelvin to mean the presence of dust and BTM (brightness temperature difference) values greater than and equal to zero degrees Kelvin to mean the absence of dust (Ackerman 1997). Although Ackerman considered the zero threshold for dust detection, this threshold can be different for different events due to ecological and environmental differences. Fig. 2 shows a schematic of the process of highlighting the dust phenomenon using the Ackerman index.

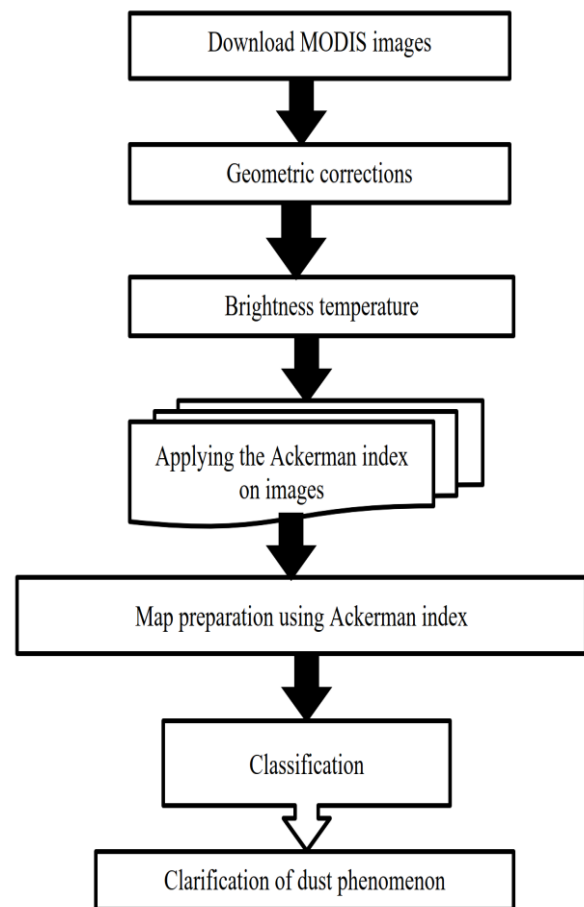


Fig. 2. Schematic of the detection of the dust phenomenon using satellite data.

2.2.4 WRF-Chem

Numerical Forecasting and Research Model of Weather with Chemistry (WRF-Chem) is included in the WRF model, Version 3. It is a research and operational model for simulating and predicting the concentration of air pollutants and particles of different sizes in the atmosphere caused by natural mechanisms and human activities (pollutants). It includes atmospheric transport and dust emission and deposition processes. The WRF-Chem model has a variety of applications from numerical prediction, evaluation studies, structural research, climate simulators, modeling of the weather system and the coupled system in the atmosphere and its modular structure, which makes the model, the quality of reception to different input data. and change be in the nature of modules. The WRF-Chem model has more advanced numerical capabilities than other models, and due to its higher resolution, it examines local effects more accurately. Unlike most chemical and dust transport models, the WRF-Chem model does not need to be paired with another atmospheric model or input atmospheric quantities because it calculates its required atmospheric quantities online. Therefore, in addition to the quantities related to atmospheric chemistry, it also provides atmospheric quantities such as wind at different levels, pressure and geopotential height as model output. The WRF-Chem modeling setup of this dust storm, and the simulated surface dust concentration, has been detailed in [Soleimani Sardo and Krakauer \(2025\)](#).

2.2.5 AOD index

The Aerosol optical depth or the optical thickness of Aerosol is a dimensionless distance that shows the amount of light beam transmission in the atmosphere and represents the absorption and scattering of aerosols in the path of light. High values of the optical thickness indicate the high accumulation of aerosols in the atmospheric column and as a result the horizontal visibility is lower. The optical thickness product of MODIS aerosol sensors is produced from the combination of two algorithms, blue deep and target dark, respectively, for bright surfaces and agricultural lands, with the aim of investigating the spatial distribution and seasonal changes of aerosol optical depth values at a wavelength of 550 nm in the study area. The target dark algorithm recovers the optical thickness data of aerosol on agricultural lands under clear weather conditions where the surface reflectance in the visible channels is 0.47 and 0.65 μm) and near infrared (1.2 μm). Meanwhile, the Blue Deep (DB) algorithm recovers the optical thickness data of aerosols on bright surfaces, taking into account the properties of dark surfaces in blue channels (0.412 and 0.47 μm) and the weak absorption of dust in the red wavelength.

3. Results and Discussion

The true color image and aerosol optical depth of the MODIS sensor of the Aqua satellite on December 19, 2016 are shown in [Fig. 3](#). The amount of AOD in the southeast region of Iran is high and it is also clear in the true color image of the dust mass over the Jazmuriyan region.

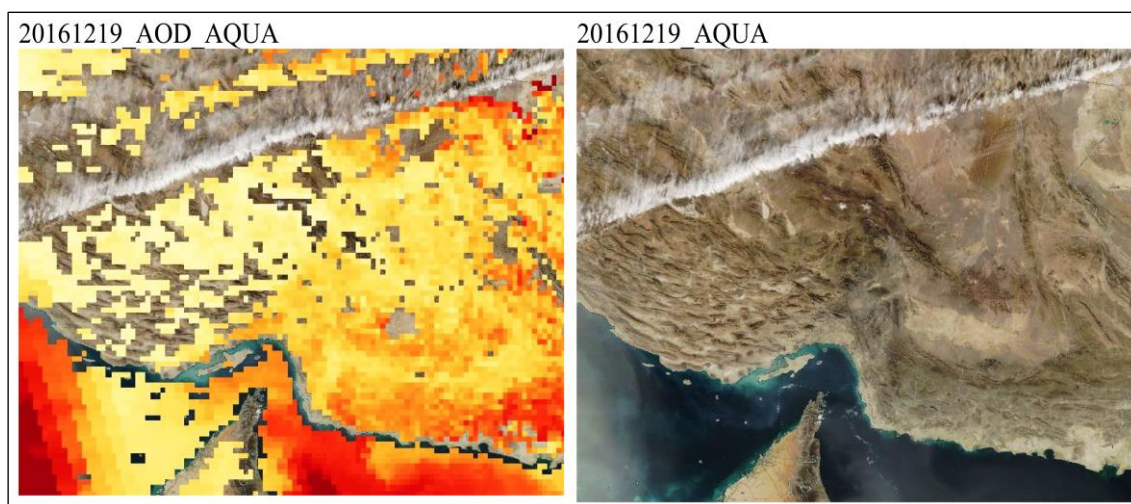


Fig. 3. MODIS sensor image of Terra and Aqua satellites.

The output of the HYSPLIT model in the forward method for December 16, 2016 at 12 UTC, which is shown in the form of a matrix with GDAS data with a horizontal resolution of 0.5 degrees with the forward method for 24 hours at an altitude of 100 meters, is shown in Fig. 4. The particles originating from this section, including the Jazmurian region, mainly moved south during this period. The AOD

values over the south of Sistan and Baluchistan province and the border between Afghanistan and Pakistan, west of the Oman Sea and east of the Persian Gulf show a significant increase compared to the previous figure. Also, the amount of this quantity has increased for the Jazmurian region and has reached 0.8 in some areas. AOD for a large part of Jazmurian region is more than 0.5 (Figs 5-16).

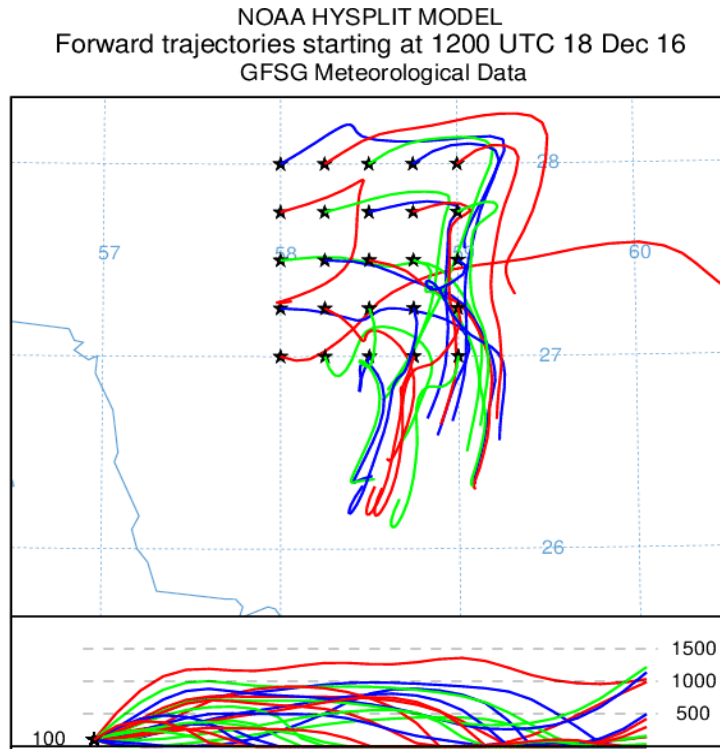


Fig. 4. The output of HYSPLIT model in the form of a matrix in the progressive method for December 16, 2016 at UTC12.

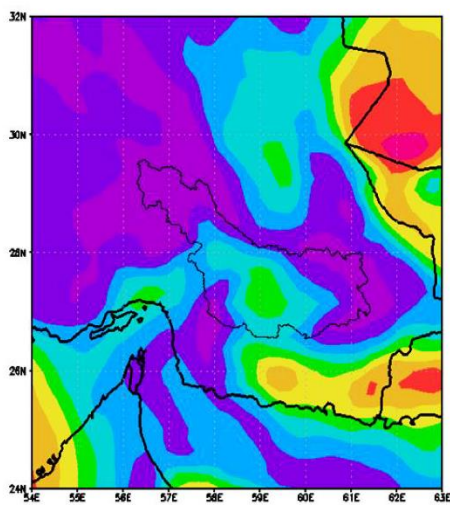


Fig. 6. Optical depth values of output particles of WRF-Chem model at UTC18 on December 17, 2016.

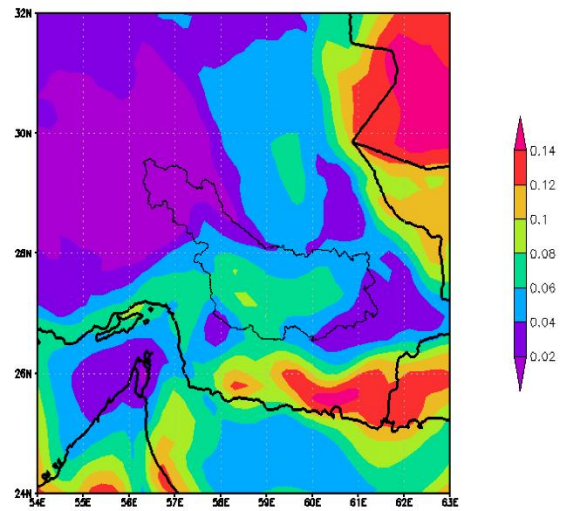


Fig. 5. Optical depth values of output particles of WRF-Chem model at UTC12 on December 17, 2016.

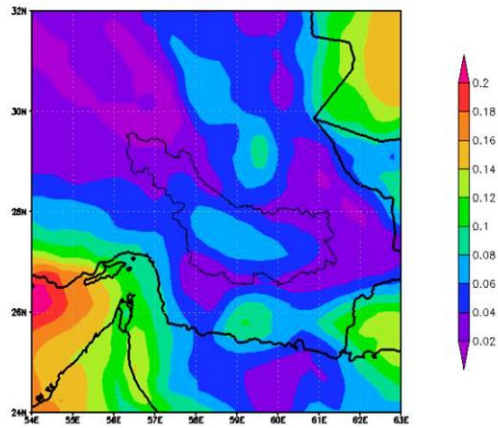


Fig. 8. Optical depth values of output particles of WRF-Chem model at UTC06 on December 18, 2016.

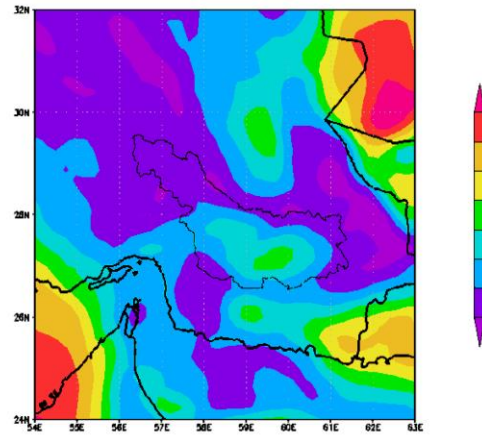


Fig. 7. Optical depth values of output particles of WRF-Chem model at UTC00 on December 18, 2016.

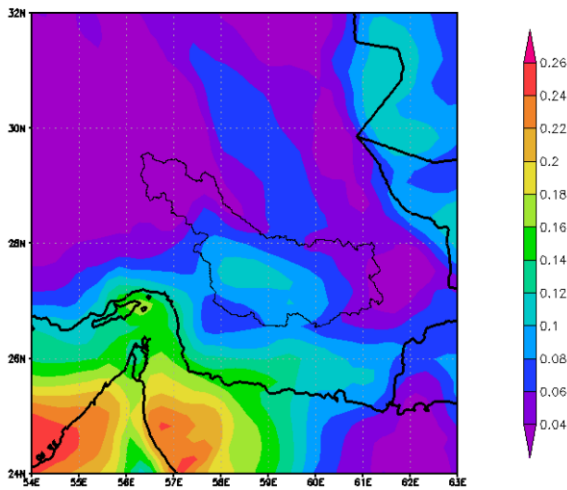


Fig. 10. Optical depth values of output particles of WRF-Chem model at UTC18 on December 18, 2016.

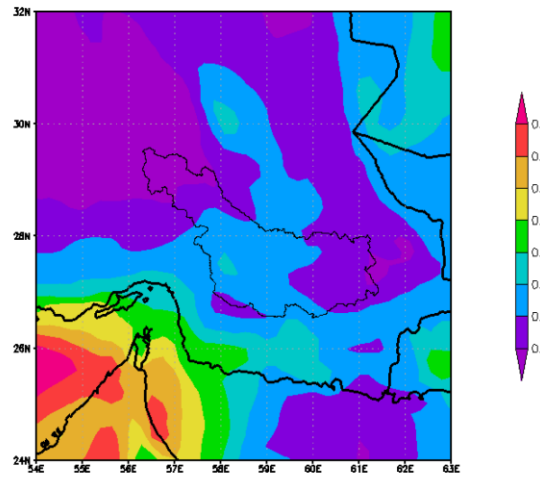


Fig. 9. Optical depth values of output particles of WRF-Chem model at UTC12 on December 18, 2016.

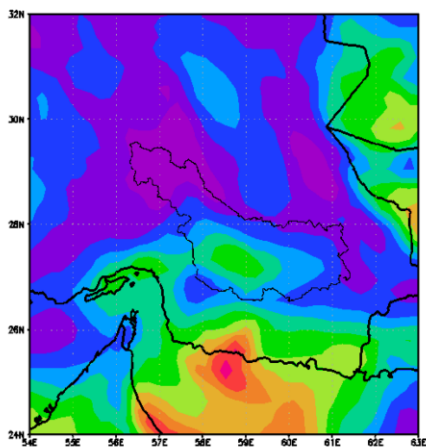


Fig. 12. Optical depth values of output particles of WRF-Chem model at UTC06 on December 19, 2016.

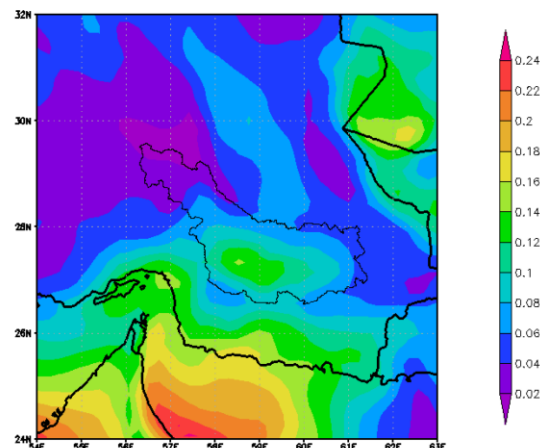


Fig. 11. Optical depth values of output particles of WRF-Chem model at UTC00 on December 19, 2016.

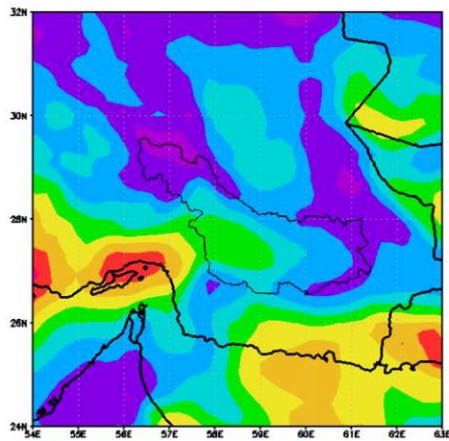


Fig. 14. Optical depth values of output particles of WRF-Chem model at UTC18 on December 19, 2016.

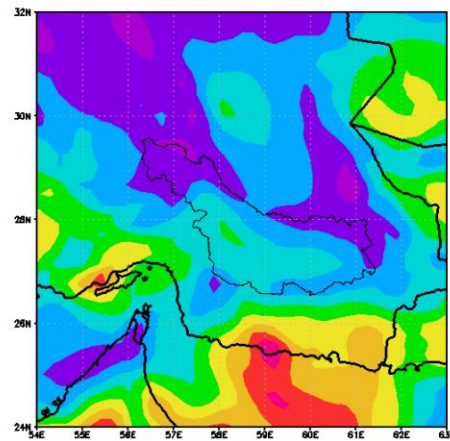


Fig. 13. Optical depth values of output particles of WRF-Chem model at UTC12 on December 19, 2016.

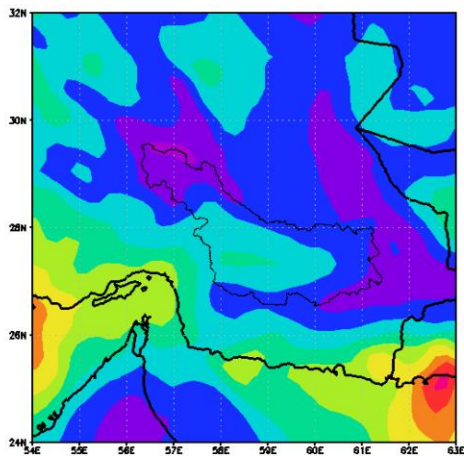


Fig. 16. Optical depth values of output particles of WRF-Chem model at UTC06 on December 20, 2016.

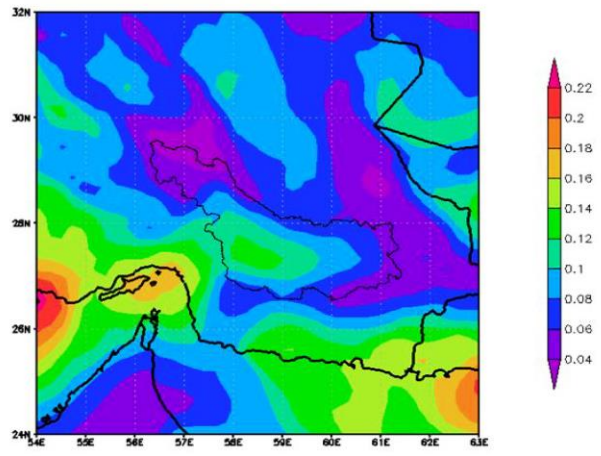


Fig. 15. Optical depth values of output particles of WRF-Chem model at UTC00 on December 20, 2016.

4. Conclusion

Simultaneous use of remote sensing satellite data with hybrid models is very valuable in dust simulation. In this research, MODIS satellite data was used, the results of which showed that the AOD level is high in the southeastern region of Iran during the case study period, and also the dust mass on the Jazmurian region is clearly visible in the true color imagery. Also, the HYSPLIT model was used for the transmission and routing of dust particles, the results of which showed that the particles originating from this section were mainly affected by the northern currents and moved towards the south. In the last step, the WRF-Chem hybrid model was used to simulate the dust storm, which numerically simulated the AOD value as well as the surface concentration of dust particles. The results showed that the AOD values on the south of Sistan and Baluchistan province and

the border between Afghanistan and Pakistan, west of the Oman Sea and east of the Persian Gulf show a significant increase compared to before. Also, the amount of this quantity has increased for the Jazmurian region and has reached 0.8 in some areas. The optical depth of particles on a large part of Jazmurian region is more than 0.5. Also, the simulated values of AOD using the WRF-Chem model in the northern parts of the area are between 0.03 and 0.04, the reason for the low value of the index in these areas can be due to the vegetation and mountainous conditions of the area. In addition, in the central parts of Jazmurian Basin, where Jazmurian Wetland is located, the value of the AOD index is always relatively high, between 0.08 and 0.16. In the central part of Jazmurian basin, almost most of the year, the soil is dry and without vegetation, and despite the dry air and also excessive livestock grazing in this area, the soil is degraded, and as a result, due to

high temperature and erosive winds, soil particles They are separated from their original bed and enter the atmosphere as suspended particles and cause dust storms in the region. Jabalbarez et al. (2023) confirm the results of this research regarding the increase of AOD in the center of Jazmurian area. Arjamand et al. (2017) introduced Jazmurian lagoon as one of the sources of dust in the southeast of the country by using the data of remote sensing and AOD index. One of the most important ways of revitalizing the Jazmurian region, which is one of the most important ecological regions in the southeast of the country, is the release of its water rights. The two big rivers, Halil River and Bampur, are the main rivers that supply the water rights of this large wetland. In the current situation, due to climatic and also human reasons (dam construction), the amount of water entering the wetland has decreased, often to zero. This wetland will become the biggest center of dust in the south of the country.

Acknowledgments

This research was supported by University of Jiroft under the grant No: 4813-02-03.

References

- Arjamand, M., Rashki, A. & Sargazi, H., 2017. Temporal and spatial monitoring of dust phenomenon using satellite data in southeast Iran, with emphasis on Jazmurian region. *Geographic Information*, 27(106), 153-168.
- Dey, S., Tripathi, S.N., Singh, R.P. & Holben, B.N., 2004. Influence of dust storms on aerosol optical properties over the Indo-Gangetic basin. *Journal of Geophysical Research: Atmospheres*, 109, D20211.
- El-Askary, H., Gautam, R., Singh, R.P. & Kafatos, M., 2006. Dust storms detection over the Indo-Gangetic basin using multi sensor data. *Advances in Space Research*, 37(4), 728-733.
- Filonchik, M., Yan, H. & Zhang, Z., 2019. Analysis of spatial and temporal variability of aerosol optical depth over China using MODIS combined Dark Target and Deep Blue product. *Theoretical and Applied Climatology*, 137(3-4), 2271-2288.
- Ginoux, P., Chin, M., Tegen, I., Prospero, J.M., Holben, B., Dubovik, O. & Lin, S.J., 2001. Sources and distributions of dust aerosols simulated with the GOCART model. *Journal of Geophysical Research: Atmospheres*, 106(D17), 20255-20273.
- Gupta P. & Sundar Christopher A. 2008. An evaluation of Terra-MODIS sampling for monthly and annual particulate matter air quality assessment over the South-eastern United States. *Atmospheric Environment*, 4, 6465-6471.
- Hamzeh, N., Fatahi, A., Zuljavadi, M., Ghaffarian, P. & Ranjbar A., 2015. Synoptic and dynamic analysis of the dust phenomenon and its simulation in the southwest of Iran in the summer of 2015. *Journal of Spatial Analysis of Environmental Hazards*. 3(1), 91-102.
- Han, X., Zhang, M., Han, Z., Xin, J. & Liu, X., 2011. Simulation of aerosol direct radiative forcing with RAMS-CMAQ in East Asia. *Atmospheric Environment*, 45(36), 6576-6592.
- Jabalbarezi, B., Zehtabian, G., Khosravi, H. & Barkhori, S., 2023. Evaluation of Temporal-Spatial Changes of Climatic Elements Affecting the Occurrence of Dust Phenomenon in Arid and Semi-arid Regions (Case Study: Jazmurian Wetland). *Environmental Erosion Research Journal*, 13(4), 109-129.
- Kalenderski, S., Stenchikov, G. & Zhao, C., 2013. Modeling a typical winter-time dust event over the Arabian Peninsula and the Red Sea. *Atmospheric Chemistry and Physics*, 13(4), 1999-2014.
- Kardan, R., Azizi, G., ZAWAR, R. P. & Mohammadi, H., 2009. Modeling the influence of water body in surrounding areas (case study: climatic modeling of Jazmoorian Watershed by creation of assumptive lake). *Iranian Journal of Watershed Management Science and Engineering*, 3(7), 15-22.
- Kargar, A., Badaq Jamali, J., Ranjbar, A. & Moinaldini, M., 2015. Numerical simulation of sandstorm and severe dust in eastern Iran using WRF-Chem model (Case study: 14 and 15 June 2012). *Journal of Environmental Science and Engineering*, 4(3), 44-35.
- Kermani, M., Taherian, E. & IZANLOO, M., 2016. Analysis of satellite images of fine dust and dust storms in Iran in order to investigate internal and external sources and their control methods. *Rahavard Salamat Magazine*, 2(1), 39-51.
- Kim, D., Chin, M., Kemp, E.M., Tao, Z., Peters-Lidard, C.D. & Ginoux, P., 2017. Development of high-resolution dynamic dust source function-A case study with a strong dust storm in a regional model. *Atmospheric Environment*, 159, 11-25.
- Li, F., Ginoux, P. & Ramaswamy, V., 2008. Distribution, transport, and deposition of mineral dust in the Southern Ocean and Antarctica: Contribution of major sources. *Journal of Geophysical Research: Atmospheres*, 113(D10).

- Mahowald, N.M., Baker, A.R., Bergametti, G., Brooks, N., Duce, R.A., Jickells, T.D. ... & Tegen, I., 2005. Atmospheric global dust cycle and iron inputs to the ocean. *Global Biogeochemical Cycles*, 19(4).
- Nabavi, S.O., Haimberger, L. & Samimi, C., 2016. Climatology of dust distribution over West Asia from homogenized remote sensing data. *Aeolian Research*, 21, 93-107.
- Negaresh, H. & Latifi, L., 2009. Geomorphological analysis of the progress of sand dunes east of Sistan plain in recent droughts. *Geography and Development*, 6(12), 43-60.
- Omidvar, K., Dehghan, M. & Khosravi, Y., 2022. Assessment of relationship between aerosol optical depth (AOD) index, wind speed, and visibility in dust storms using genetic algorithm in central Iran (case study: Yazd Province). *Air Quality, Atmosphere & Health*, 15(10), 1745-1753.
- Prasad, A.K., Singh, R.P. & Singh, A., 2004. Variability of aerosol optical depth over Indian subcontinent using MODIS data. *Journal of the Indian Society of Remote Sensing*, 32(4), 313-316.
- Prasad, A.K., Singh, S., Chauhan, S.S., Srivastava, M.K., Singh, R.P. & Singh, R., 2007. Aerosol radiative forcing over the Indo-Gangetic plains during major dust storms. *Atmospheric Environment*, 41(29), 6289-6301.
- Prospero, J.M., Ginoux, P., Torres, O., Nicholson, S. E. & Gill, T.E., 2002. Environmental characterization of global sources of atmospheric soil dust identified with the Nimbus 7 Total Ozone Mapping Spectrometer (TOMS) absorbing aerosol product. *Reviews of Geophysics*, 40(1), 2-1.
- Prospero, J.M. & Lamb, J.P., 2003. African droughts and dust transport to the Caribbean: climate change and implications. *Science*, 302, 1024-1027.
- Rajaei, T., Rohani, N., Jabbari, E. & Mojaradi, B. , 2020. Tracing and assessment of simultaneous dust storms in the cities of Ahvaz and Kermanshah in western Iran based on the new approach. *Arabian Journal of Geosciences*, 13(12), 461.
- Rizza, U., Miglietta, M.M., Mangia, C., Ielpo, P., Morichetti, M., Iachini, C. ... & Passerini, G., 2018. Sensitivity of WRF-Chem model to land surface schemes: Assessment in a severe dust outbreak episode in the Central Mediterranean (Apulia Region). *Atmospheric Research*, 201, 168-180.
- Soleimani Sardoo, F. & Krakauer, N., 2025. Surface concentration values simulation using WRF models and GOCART scheme in southeast Iran (Case study: December 16-20, 2016 storm), *Sustainable Earth Trends*, 5(2), 1-10.
- Tavakoli Neko, H., Pourmeidani, A. & Adnani M., 2024. Detection and tracking of dust phenomena and determination of its origin using AOD index obtained from MODIS sensor data in Qom province. *Journal of RS and GIS for Natural Resources*, 15(2), 54-70.
- Tegen, I. & Fung, I., 1994. Modeling of mineral dust in the atmosphere: Sources, transport, and optical thickness. *Journal of Geophysical Research: Atmospheres*, 99(D11), 22897-22914.
- Uno, I., Wang, Z., Chiba, M., Chun, Y.S., Gong, S. L., Hara, Y. ... & Westphal, D.L., 2006. Dust model intercomparison (DMIP) study over Asia: Overview. *Journal of Geophysical Research: Atmospheres*, 111(D12).
- Zhao, C., Liu, X., Leung, L.R., Johnson, B., McFarlane, S.A., Gustafson Jr, W.I. ... & Easter, R., 2010. The spatial distribution of mineral dust and its shortwave radiative forcing over North Africa: modeling sensitivities to dust emissions and aerosol size treatments. *Atmospheric Chemistry and Physics*, 10(18), 8821-8838.
- Zhao, C., Liu, X., Ruby Leung, L. & Hagos, S., 2011. Radiative impact of mineral dust on monsoon precipitation variability over West Africa. *Atmospheric Chemistry and Physics*, 11(5), 1879-1893.